PNAS

Main Manuscript for

Exacerbated atherosclerosis in progeria is prevented by progerin elimination in vascular smooth muscle cells but not endothelial cells

Ignacio Benedicto[1,2], Rosa María Carmona[2], Ana Barettino[2,3], Carla Espinós-Estévez[2,3], Pilar Gonzalo[2,3], Rosa M. Nevado[2,3], Miguel de la Fuente-Pérez[2], María J. Andrés-Manzano[2,3], Cristina González-Gómez[2,3], Loïc Rolas[4], Beatriz Dorado[2,3], Sussan Nourshargh[4], Magda R. Hamczyk[3,5], Vicente Andrés[2,3*].

1. Centro de Investigaciones Biológicas Margarita Salas (CIB), Consejo Superior de Investigaciones Científicas (CSIC), 28040 Madrid, Spain.
2. Centro Nacional de Investigaciones Cardiovasculares (CNIC), 28029 Madrid, Spain.
3. CIBER en Enfermedades Cardiovasculares (CIBERCV), Madrid, Spain.
4. William Harvey Research Institute, Faculty of Medicine and Dentistry, Queen Mary University of London, London E1 4NS, United Kingdom.
5. Departamento de Bioquímica y Biología Molecular, Instituto Universitario de Oncología (IUOPA), Universidad de Oviedo, 33006 Oviedo, Spain.

*Corresponding author
Email: vandres@cnic.es

Author Contributions: I.B. and V.A. designed research; I.B., R.M.C., A.B., C.E.-E., P.G., R.M.N., M.F.-P., M.J.A-M., and C.G.-G performed research; L.R. and S.N. contributed new reagents/analytic tools; I.B., B.D., and M.R.H. analyzed data; I.B. and V.A. wrote the paper; all authors revised manuscript.

Competing Interest Statement: No competing interests.

Classification: Biological Sciences (Cell Biology).

Keywords: Hutchinson-Gilford progeria syndrome, atherosclerosis, vascular smooth muscle cells, endothelial cells.

This file includes:

Main Text
Figures 1 to 2

Abstract

Hutchinson-Gilford progeria syndrome (HGPS) is a rare disease caused by the expression of progerin, a mutant protein that accelerates aging and precipitates death. Given that atherosclerosis complications are the main cause of death in progeria, here we investigated whether progerin-induced atherosclerosis is prevented in *HGPSrev-Cdh5-CreERT2* and *HGPSrev-SM22α-Cre* mice with progerin suppression in endothelial cells (ECs) and vascular smooth muscle cells (VSMCs), respectively. *HGPSrev-Cdh5-CreERT2* mice were undistinguishable from *HGPSrev* mice with ubiquitous progerin expression, in contrast with the ameliorated progeroid phenotype of *HGPSrev-SM22α-Cre* mice. To study atherosclerosis, we generated atheroprone mouse models by overexpressing a PCSK9 gain-of-function mutant. While *HGPSrev-Cdh5-CreERT2* and *HGPSrev* mice developed a similar level of excessive atherosclerosis, plaque development in *HGPSrev-SM22α-Cre* mice was reduced to wild-type levels. Our studies demonstrate that progerin suppression in VSMCs, but not in ECs, prevents exacerbated atherosclerosis in progeroid mice.

Hutchinson-Gilford progeria syndrome (HGPS) is a rare genetic disorder caused by a heterozygous mutation in the *LMNA* gene that provokes wide expression of progerin, a mutant version of the nuclear protein lamin A that accelerates aging and precipitates death (average lifespan: 14.6 years). Patients develop severe atherosclerosis, which in most cases leads to fatal myocardial infarction, stroke, or heart failure (1).

Gene editing has emerged as a promising approach to reducing progerin expression (2–5). To optimize gene therapy in HGPS, it is important to identify the appropriate time window for intervention and the cell types in which progerin elimination yields more benefit. To tackle these questions, we previously generated progeroid *HGPSrev* mice which ubiquitously express progerin, lack lamin A, and allow time- and cell type-specific progerin suppression and lamin A restoration (6) (see SI Appendix). Here we investigated whether HGPS-associated atherosclerosis is prevented upon progerin suppression and lamin A restoration in endothelial cells (ECs) or vascular smooth muscle cells (VSMCs), key vascular cell types in atherogenesis.

Results and Discussion

We generated *HGPSrev-Cdh5-CreERT2* mice with EC-specific progerin elimination and lamin A restoration. We treated wild-type (*WT*), *HGPSrev*, and *HGPSrev-Cdh5-CreERT2* mice with tamoxifen at 1.5 months of age, long before the first HGPS-like signs in *HGPSrev* mice, and analyzed progerin expression in 12-month-old mice. Immunofluorescence assays confirmed efficient progerin elimination in luminal ECs in *HGPSrev-Cdh5-CreERT2* aorta (Fig. 1A), and EC-specific progerin suppression in *HGPSrev-Cdh5-CreERT2* aorta, heart, liver, and kidney (Fig. 1B). RT-qPCR analysis confirmed progerin suppression and lamin A restoration in ECs but not macrophages from *HGPSrev-Cdh5-CreERT2* hearts (Fig. 1C).

HGPSrev-Cdh5-CreERT2 mice had the characteristic alterations of *HGPSrev* mice with ubiquitous progerin expression, including body-weight loss, premature death, aortic VSMC loss, and exaggerated medial collagen deposition (Fig. 1D, E). *HGPSrev* mice showed increased leukocyte accumulation in the aortic intima compared with *WT* controls, which was not significantly reduced in *HGPSrev-Cdh5-CreERT2* mice (Fig. 1F). We studied the effects of progerin suppression and lamin A restoration in ECs after inducing atherosclerosis by intravenous injection of an adeno-associated virus encoding the mouse PCSK9 gain-of-function mutant $PCSK9^{D377Y}$ (rAAV8-m$PCSK9^{D377Y}$) followed by 2 months of high-fat diet (HFD) (7) (Fig. 1G). Total cholesterol and low-density lipoprotein (LDL) serum concentrations were markedly higher in all genotypes post-HFD compared with baseline (Fig. 1H), and the concentration of circulating white blood cells at endpoint was similar among genotypes (Fig. 1I). Consistent with our previous studies in other atherosclerosis-susceptible HGPS mouse models with ubiquitous progerin expression (8, 9), aortic atherosclerosis burden was higher in *HGPSrev* mice than in *WT* controls, but this excess of atherosclerosis also occurred upon EC-specific progerin suppression and lamin A restoration (Fig. 1J).

We previously demonstrated that *HGPSrev-SM22α-Cre* mice show efficient progerin suppression and lamin A restoration in VSMCs and cardiomyocytes, which prevents HGPS-associated VSMC loss, vascular fibrosis, and premature death (6). We used this model to assess whether suppressing progerin in arterial VSMCs had any effect on vascular inflammation and atherosclerosis. *HGPSrev-SM22α-Cre* mice showed reduced leukocyte accumulation in the aortic intima compared with *HGPSrev* mice with ubiquitous progerin expression (Fig. 2A). $PCSK9^{D377Y}$ overexpression and HFD (Fig. 2B) increased total cholesterol and LDL serum concentrations in all genotypes, which showed similar concentrations of circulating white blood cells at endpoint (Fig. 2C, D). Atheroprone *HGPSrev-SM22α-Cre* mice did not show aortic VSMC loss or medial fibrosis (Fig. 2E) and their atherosclerosis burden was indistinguishable from that in *WT* mice (Fig. 2F).

Although further work is needed to provide mechanistic insights, our studies in *HGPSrev* mice show that progerin suppression and lamin A restoration in VSMCs, but not in ECs, prevents HGPS-associated exacerbated atherosclerosis, the main driver of premature death in HGPS patients, suggesting that selective VSMC targeting in gene-editing therapies to correct the HGPS-instigating mutation may yield significant therapeutic benefit. Such a strategy would likely require lower doses of gene-editing reagents than those needed for systemic progerin suppression, which may increase opportunities for clinical applications.

Materials and Methods

HGPSrev-Cdh5-CreERT2 mice were generated by crossing *HGPSrev* (6) and *Tg(Cdh5-cre/ERT2)1Rha* mice (MGI ID 3848982). *HGPSrev-SM22α-Cre* mice (6) and PCSK9^{D377Y}-induced atherosclerosis (7) were previously described. Progerin levels were quantified by immunofluorescence analysis of several tissues and RT-qPCR on sorted cardiac cells. Cellular content and collagen accumulation in the aortic media were analyzed by hematoxylin-eosin and Masson's trichrome staining, respectively. Atherosclerosis was quantified by *en face* oil red O staining of aortas. Details provided in SI Appendix.

Acknowledgments

We thank R.H. Adams for *Tg(Cdh5-cre/ERT2)1Rha* mice, J.F. Bentzon for rAAV8-mPCSK9^{D377Y}, and S. Bartlett for English editing. Aorta and mouse icons made with BioRender.com licensed to V.A. Work supported by grant PID2022-141211OB-I00 funded by MICIU/AEI/10.13039/501100011033 and ERDF/EU to V.A. I.B. supported by Comunidad de Madrid (2017-T1/BMD-5247, 2021-5A/BMD-20944) with co-funding from the European Structural and Investment Fund, RYC2021-033805-I (MICIU/AEI/10.13039/501100011033, European Union NextGenerationEU/PRTR), and PID2022-137111OA-I00 (MICIU/AEI/10.13039/501100011033, ERDF/EU). Salary support to A.B. (BES-2017-079705, MICIU/AEI/10.13039/501100011033, ESF), C.E.-E. (Fundación "la Caixa", LCF/BQ/DR19/1170012), R.M.N (Ministerio de Educación, Cultura y Deporte, FPU16/05027), and M.R.H. (MICIU, IJC2019-040798-I). The CNIC is supported by Instituto de Salud Carlos III (ISCIII), Ministerio de Ciencia, Innovación y Universidades (MICIU), Pro-CNIC Foundation, and is a Severo Ochoa Center of Excellence (grant CEX2020-001041-S funded by MICIU/AEI/10.13039/501100011033). Generation of anti-progerin antibody funded by Wellcome Trust (098291/Z/12/Z, 221699/Z/20/Z). Microscopy and Dynamic Imaging Unit-CNIC/ICTS-ReDib supported by ICTS-2018-04-CNIC-16 funded by MICIU/AEI/10.13039/501100011033 and ERDF–A way to make Europe.

References

1. L. B. Gordon, W. T. Brown, F. S. Collins, "Hutchinson-Gilford Progeria Syndrome" in *GeneReviews((R))*, M. P. Adam, *et al.*, Eds. (1993).

2. O. Santiago-Fernandez, *et al.*, Development of a CRISPR/Cas9-based therapy for Hutchinson-Gilford progeria syndrome. *Nat Med* **25**, 423–426 (2019).

3. E. Beyret, *et al.*, Single-dose CRISPR-Cas9 therapy extends lifespan of mice with Hutchinson-Gilford progeria syndrome. *Nat Med* **25**, 419–422 (2019).

4. L. W. Koblan, *et al.*, In vivo base editing rescues Hutchinson-Gilford progeria syndrome in mice. *Nature* **589**, 608–614 (2021).

5. D. Whisenant, *et al.*, Transient expression of an adenine base editor corrects the Hutchinson-Gilford progeria syndrome mutation and improves the skin phenotype in mice. *Nat Commun* **13**, 3068 (2022).

6. A. Sanchez-Lopez, *et al.*, Cardiovascular Progerin Suppression and Lamin A Restoration Rescue Hutchinson-Gilford Progeria Syndrome. *Circulation* **144**, 1777–1794 (2021).

7. M. M. Bjørklund, *et al.*, Induction of atherosclerosis in mice and hamsters without germline genetic engineering. *Circ Res* **114**, 1684–9 (2014).

8. M. R. Hamczyk, *et al.*, Vascular Smooth Muscle-Specific Progerin Expression Accelerates Atherosclerosis and Death in a Mouse Model of Hutchinson-Gilford Progeria Syndrome. *Circulation* **138**, 266–282 (2018).

9. R. M. Nevado, M. R. Hamczyk, P. Gonzalo, M. J. Andres-Manzano, V. Andres, Premature Vascular Aging with Features of Plaque Vulnerability in an Atheroprone Mouse Model of Hutchinson-Gilford Progeria Syndrome with Ldlr Deficiency. *Cells* **9** (2020).

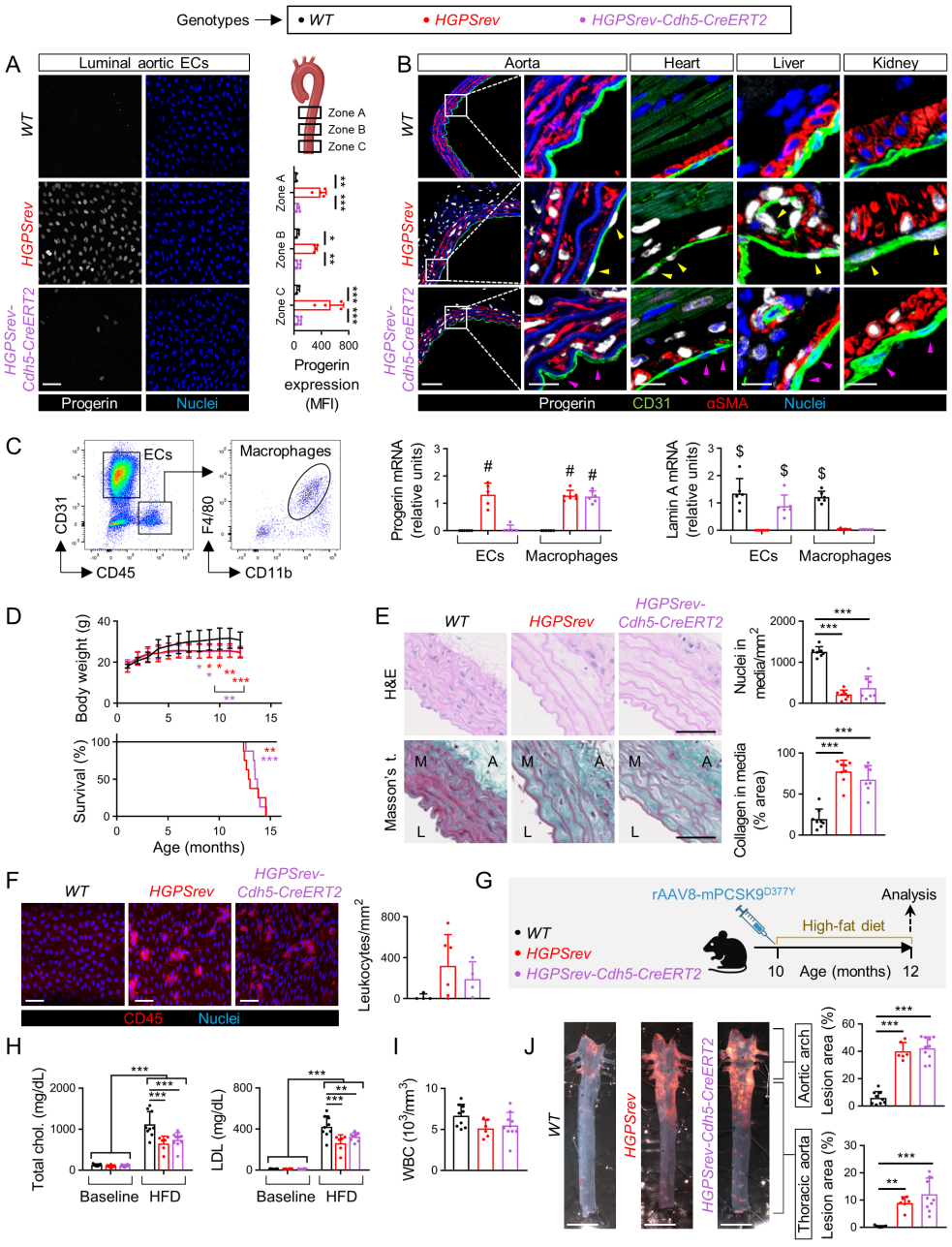

Figure 1. Endothelium-specific progerin suppression and lamin A restoration do not prevent body weight reduction, lifespan shortening, and excessive atherosclerosis. (*A*) *En face* immunofluorescence in 3 different zones of thoracic aortas showing progerin (white) and nuclei (blue) in luminal ECs (*WT,* n=2; *HGPSrev* and *HGPSrev-Cdh5-CreERT2*, n=4). Bar, 50 μm. MFI, mean fluorescence intensity. **(*B*)** Immunofluorescence on tissue cross-sections showing progerin (white), CD31 (green), αSMA (red), and nuclei (blue) (n=4). Bar in aorta (left), 50 μm; bar in zoomed aorta and heart, liver, and kidney, 10 μm. Yellow and pink arrowheads indicate progerin-positive and progerin-negative ECs, respectively. **(*C*)** *Left:* Gating strategy for the isolation of mouse cardiac ECs and macrophages by cell sorting. *Right:* RT-qPCR analysis of

progerin and lamin A mRNA expression in cardiac ECs and macrophages (n=5-6). #, p<0.001 *vs*. ECs from *WT* and *HGPSrev-Cdh5-CreERT2* mice and macrophages from *WT* mice. $, p<0.001 *vs*. ECs from *HGPSrev* mice and macrophages from *HGPSrev* and *HGPSrev-Cdh5-CreERT2* mice. **(*D*)** *Top*: Body weight (*WT,* n=13; *HGPSrev* and *HGPSrev-Cdh5-CreERT2,* n=8). *Bottom*: Kaplan-Meier survival curves (*WT* n=5; *HGPSrev* and *HGPSrev-Cdh5-CreERT2*, n=8). Red and purple asterisks indicate significant differences between *WT* and *HGPSrev* or *HGPSrev-Cdh5-CreERT2* mice, respectively. **(*E*)** Hematoxylin-eosin (H&E) and Masson's trichrome (Masson's t.) staining of aortic arch sections (n=7-8). Bars, 50 µm. L, lumen; M, media; A, adventitia. ***(F)*** *En face* immunofluorescence of the luminal surface of thoracic aortas showing CD45 (red) and nuclei (blue) (*WT,* n=4; *HGPSrev*, n=6; *HGPSrev-Cdh5-CreERT2*, n=4). Bars, 50 µm. **(*G*)** Protocol for atherosclerosis studies. **(*H*)** Total cholesterol (chol.) and LDL serum levels (n=6-14). **(*I*)** Circulating white blood cells (WBC) (n=6-10). (***J***) *En face* oil red O staining of aortas (n=6-10). Bars, 5 mm.

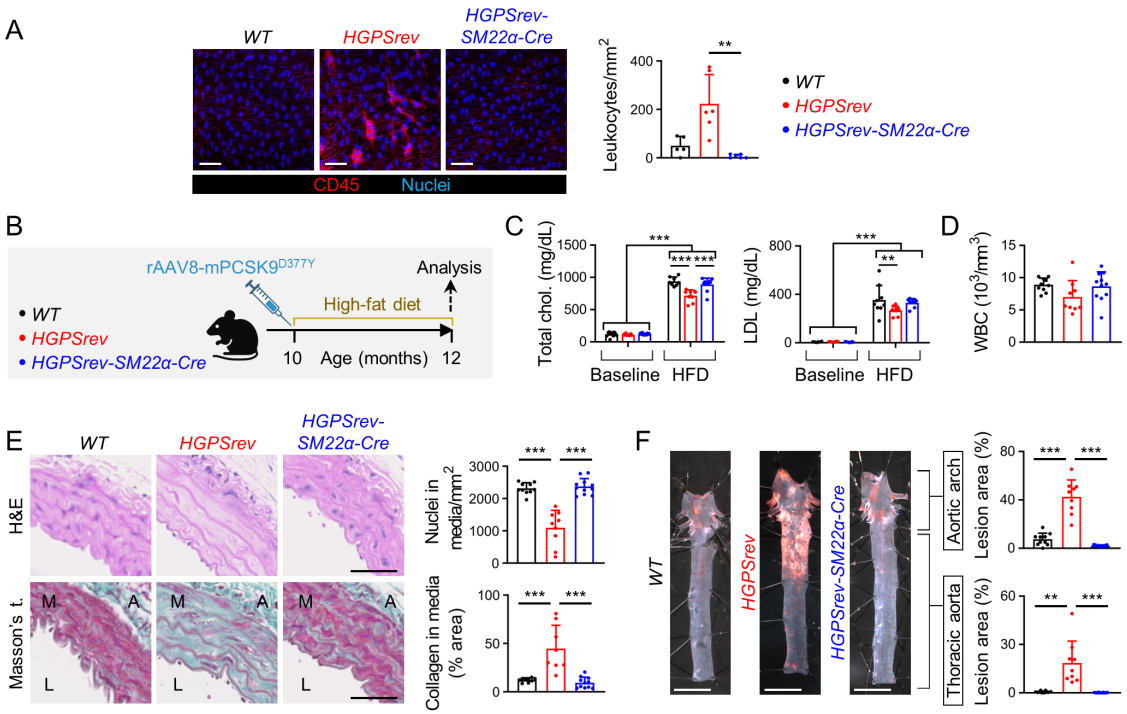

Figure 2. Progerin elimination and lamin A restoration in VSMCs prevent excessive atherosclerosis. ***(A)*** *En face* immunofluorescence of the luminal surface of thoracic aortas showing CD45 (red) and nuclei (blue) (*WT,* n=5; *HGPSrev* and *HGPSrev-SM22α-Cre*, n=6). Bars, 50 μm. **(*B*)** Protocol for atherosclerosis studies. **(*C*)** Total cholesterol (chol.) and LDL serum levels (n=8-11). **(*D*)** Circulating white blood cells (WBC) (n=9-11). **(*E*)** Hematoxylin-eosin (H&E) and Masson's trichrome (Masson's t.) staining of aortic arch sections (n=8-11). Bars, 50 μm. L, lumen; M, media; A, adventitia. **(*F*)** *En face* oil red O staining of aortas (n=9-11). Bars, 5 mm.

PNAS

Supporting Information for

Exacerbated atherosclerosis in progeria is prevented by progerin elimination in vascular smooth muscle cells but not endothelial cells

Ignacio Benedicto, Rosa María Carmona, Ana Barettino, Carla Espinós-Estévez, Pilar Gonzalo, Rosa M. Nevado, Miguel de la Fuente-Pérez, María J. Andrés-Manzano, Cristina González-Gómez, Loïc Rolas, Beatriz Dorado, Sussan Nourshargh, Magda R. Hamczyk, Vicente Andrés.

Corresponding author: Vicente Andrés
Email: vandres@cnic.es

This PDF file includes:

Supplementary Materials and Methods

Mice

We previously generated progeroid *HGPSrev* mice, which ubiquitously express progerin, lack lamin A, and allow time- and cell type-specific progerin suppression and lamin A restoration upon Cre activation (1). The lack of lamin A in homozygous *HGPSrev* mice does not fully recapitulate the *LMNA* expression pattern in HGPS patients, who carry in heterozygosis the mutant *LMNA* allele and therefore express both lamin A and progerin (2, 3). However, several studies have shown that the lack of lamin A is not detrimental in mice expressing lamin C (4–6), another *LMNA* isoform whose expression is not affected by the HGPS-causing mutation. Like HGPS patients, homozygous *HGPSrev* mice appear normal at birth. The first HGPS-like sign in *HGPSrev* mice is weight loss, appearing from ≈6 months of age, followed by progressive vascular smooth muscle cell (VSMC) loss, vascular fibrosis, lipodystrophy, cardiovascular alterations, and premature death (1). This is also the case for homozygous $Lmna^{G609G/G609G}$ mice (4), the most frequently used animal model for HGPS research, which expresses progerin, lamin C, and only residual levels of lamin A. Remarkably, homozygous *HGPSrev* and $Lmna^{G609G/G609G}$ mice are phenotypically very similar to homozygous G608G BAC mice, another HGPS model that expresses human lamin A, lamin C, and progerin together with endogenous mouse lamin A and lamin C (7, 8). Collectively, these findings indicate that progerin expression in mice induces a human-like HGPS phenotype that is qualitatively similar both in the absence or presence of different levels of concomitant lamin A expression.

HGPSrev-Cdh5-CreERT2 mice were generated by crossing *HGPSrev* (1) and *Tg(Cdh5-cre/ERT2)1Rha* mice (MGI ID 3848982) (9). *HGPSrev-SM22α-Cre* mice were generated as previously described (1). For experiments shown in Fig. 1, *WT*, *HGPSrev*, and *HGPSrev-Cdh5-CreERT2* mice were injected intraperitoneally at 1.5 months of age with 0.2 mg g^{-1} tamoxifen (T5648, Sigma) in corn oil (C8267, Sigma) for 3 consecutive days. Mice were housed in a specific pathogen-free facility in individually ventilated cages with 12 h light/12 h dark cycles at a temperature of 22 ± 2 °C and 50% relative humidity (range 45%–60%). Mice had *ad libitum* access to water and food (D184, SAFE, and Rod18-A, LASQCdiet). Where indicated, mice were fed a high-fat diet containing 10.7% total fat and 0.75% cholesterol (S9167-E011, Ssniff). Males and females were included in all experiments. All experimental mice were on the C57BL/6J genetic background, and all analyses were carried out by operators blinded to genotype. Mice were euthanized by CO_2 inhalation except in experiments shown in Figs. 1A, 1F, and 2A where anesthetized animals were perfused with 4% PFA. All animal procedures followed EU Directive 2010/63/EU and Recommendation 2007/526/EC, enacted in Spain under Real Decreto 53/2013 and 191/2013. Animal protocols were approved by the local ethics committees and the Animal Protection Area of the Comunidad Autónoma de Madrid (PROEX 105.0/22).

Aorta *en face* immunostaining and quantitative image analysis

En face immunofluorescence studies in aortic tissue from 12-month-old mice were done as previously described (10) using a progerin-specific antibody (1) (1:800), biotinylated mouse anti-mouse CD45.2 (1:200, 553771, BD Biosciences), goat anti-rabbit IgG H&L Alexa Fluor 647 (1:400, A21245, Thermo Fisher Scientific), streptavidin Cyanine Cy3 (1:200, 016-160-084, Jackson ImmunoResearch), and Hoechst 33342 (10 μM, B2261, Sigma) as indicated. Images were acquired with an LSM 700 confocal microscope equipped with a LD LCI Plan-Apochromat 25x/0.8 Imm Korr DIC M27 objective (Zeiss). In Fig. 1A the analysis was carried out in 3 different zones along the thoracic aorta, quantifying 3 25x fields per zone using ImageJ Fiji software (11). Nuclei from luminal ECs (72-173 nuclei per field) were selected based on Hoechst 33342 staining, and mean fluorescence intensity of nuclear progerin was quantified from a sum projection of z sections. In Figs. 1F and 2A $CD45^+$ leukocyte accumulation was analyzed in one zone of the thoracic aorta, quantifying 3 25x fields in each mouse.

Immunostaining of tissue sections

Twelve-month-old mice were anesthetized and perfused through the left ventricle with 4% PFA in PBS for 5 min. Tissues were fixed with 4% PFA in PBS, dehydrated to xylene, embedded in paraffin, and cut into 5-µm sections using a microtome (RM2245, Leica). Heart, liver, and kidney sections were incubated 1 h at room temperature (RT) in 100 mM glycine. Antigens were retrieved with 10 mM sodium citrate buffer (pH 6) and samples were blocked for 1 h at RT with 0.3% Triton X-100, 5% BSA, and 5% normal goat serum in PBS. Primary and secondary antibodies were diluted in PBS supplemented with 0.3% Triton X-100, 5% BSA, and 2.5% normal goat serum. After overnight incubation at 4ºC with antibodies targeting progerin (1) (1:800) and CD31 (1:50, DIA-310, Dianova), samples were incubated for 2 h at RT with goat anti-rabbit IgG Affinipure Fab Fragment Alexa Fluor 647 (1:500, 111-607-008, Jackson ImmunoResearch), goat anti-Rat IgG (H+L) Alexa Fluor 488 (1:500, A11006, Thermo Fisher Scientific), and anti–smooth muscle α-actin-Cy3 (1:200, C6198, Sigma). Sections were incubated with DAPI (1:5,000, D23842, Invitrogen) for 30 min at RT and mounted in Fluoromount G imaging medium (00-4958-02, Thermo Fisher Scientific). Images were acquired with an LSM 700 confocal microscope equipped with a LD LCI Plan-Apochromat 25x/0.8 Imm Korr DIC M27 objective (Zeiss).

Quantification of progerin and lamin A mRNA expression in cardiac ECs and macrophages

Twelve-month-old mice were euthanized and carefully perfused through the left ventricle with 10 ml cold PBS. Heart apexes were minced and digested at 37°C for 15 min in serum-free DMEM supplemented with digestion buffer [4 × stock: 25 mg ml^{-1} collagenase A (Roche), 25 mg ml^{-1} dispase II (Roche), 250 µg ml^{-1} DNase (Roche), 140 mM NaCl, 5 mM KCl, 2.5 mM phosphate buffer, 10 mM HEPES, 2 mM $CaCl_2$, and 1.3 mM $MgCl_2$]. Digested tissue was thoroughly pipetted and filtered through a 70-µm cell strainer. Cell suspensions were pelleted at 400×g for 5 min at 4ºC and resuspended in sorting buffer (PBS supplemented with 1% FBS, 2 mM EDTA, 5 mM glucose, and 10 mM HEPES) including a CD16/CD32 antibody to block Fc receptors (1:200, 101302, Biolegend). Cells were stained with anti-CD31 Alexa Fluor 647 (1:200, 102416, Biolegend), anti-CD45 Pacific Blue (1:200, 103126, Biolegend), anti-CD11b FITC (1:200, AGEL0306, AssayGenie), and anti-F4/80 PE/Cy7 (1:100, 123114, Biolegend) for 30 min on ice. Cells were washed with cold sorting buffer, pelleted at 400×g for 5 min at 4ºC, resuspended in cold sorting buffer, filtered through a 70-µm cell strainer, and stained with 1 µg ml^{-1} propidium iodide (P4864, Sigma). Viable cardiac ECs ($PI^-CD31^+ CD45^-$) and macrophages ($PI^-CD31^- CD45^+ CD11b^+ F4/80^+$) were isolated by cell sorting (FACSAria Cell Sorter, BD Biosciences) and collected in 750 µl TRI Reagent Solution (AM9738, Invitrogen). RNA was extracted following the manufacturer's instructions until phase separation, when the aqueous phase was diluted 1:1 with 70% ethanol and loaded in two steps into a column of the RNeasy Mini Kit (Qiagen). RNA was purified following the manufacturer's instructions and cDNA was prepared with the High-Capacity cDNA Reverse Transcription Kit (Applied Biosystems). Real-time qPCR was carried out in a Bio Rad-CFX384 Real-Time PCR System (Bio Rad) using PowerSYBR Green PCR Master Mix (Thermo Fisher Scientific) and the following primers: progerin, 5'-tgagtacaacctgcgctcac-3' (*Lmna* exon 11) and 5'-agatggctggcaactagaag-3' (BGH polyA from the *HGPSrev* cassette); lamin A, 5'-tcacagtcactcgaagcttc-3' (*Lmna* exon 11, region absent in progerin) and 5'-ggtcccagattacatgatgc-3' (*Lmna* exon 12); *Gapdh* (for normalization using the $2^{-\Delta\Delta Ct}$ method), 5'-aaatggtgaaggtcggtgtg-3' and 5'-gagtggagtcatactggaac-3'. All qPCR reactions were performed in technical duplicates.

Generation of atheroprone mouse models

The $PCSK9^{D377Y}$ model is one of the options for atherosclerosis studies mentioned in a scientific statement on atherosclerosis animal studies from the American Heart Association (12). This system induces atherosclerosis mainly via LDL receptor downregulation and concomitant increase in serum cholesterol levels (13). An advantage of the $PCSK9^{D377Y}$ model is that it avoids the generation of new mouse lines, therefore reducing the number of animals needed to comply with the 3Rs principles (replacement, reduction, and refinement). Adeno-associated virus encoding mouse $PCSK9^{D377Y}$ (rAAV8-m$PCSK9^{D377Y}$) (14) was prepared, purified by iodixanol gradient, and titrated by qPCR at CNIC Viral Vectors Unit. For atherosclerosis studies, 10-month-old *WT*, *HGPSrev, HGPSrev-Cdh5-CreERT2*, and *HGPSrev-SM22α-Cre* mice were transduced with a single dose of rAAV8-m$PCSK9^{D377Y}$ viral particles (10^{11} in 100 µl PBS, administered by intravenous

tail injection), and then were fed a high-fat diet containing 10.7% total fat and 0.75% cholesterol (S9167-E011, Ssniff) from the day after transduction until sacrifice at 12 months of age.

Atherosclerosis quantification and histological studies
Aortic atherosclerosis burden in 12-month-old mice was quantified after staining with 0.2% oil red O (ORO, O0625, Sigma) (15, 16). VSMC number and collagen content in the medial layer of the aortic arch were quantified after staining with hematoxylin-eosin or Masson's trichrome, respectively (15, 16).

Hematology and biochemical analyses
Mouse blood was collected by submandibular bleeding (10-month-old mice, baseline in Fig. 1H and 2C) or cardiac puncture (at endpoint). For hematological tests, samples were collected in Microvette 100 EDTA tubes (Sarstedt) and analyzed with a PENTRA 80 hematology analyzer (Horiba). For serum cholesterol and LDL analysis, blood was collected in plastic tubes, incubated at RT to allow clotting, and centrifuged at 1,900×g and 4°C for 10 min. Serum was centrifuged at 4°C for 10 additional min at maximum speed before analysis. The serum concentration of total cholesterol and LDL was measured using a Dimension RxL Max Integrated Chemistry System (Siemens Healthineers). All analyses were performed by specialized staff at CNIC Animal Facility.

Statistical analysis
All data are presented as mean+standard deviation. Statistical significance (unless stated otherwise in the figure legend): *, $p<0.05$; **, $p<0.01$; ***, $p<0.001$. Body weight analysis was carried out with a mixed effects model with the Geisser–Greenhouse correction and Tukey's multiple comparison test (Fig. 1D). Survival analysis was carried out with the Mantel–Cox test (Fig. 1D). For data with one independent variable, we used one-way ANOVA plus Tukey's multiple comparisons test for normally distributed data [Fig. 1E, I, J; Fig. 2D, E, F (aortic arch)], and the Kruskal-Wallis test plus Dunn's multiple comparisons test for non-normally distributed data [Fig. 1F; Fig. 2A, 2F (thoracic aorta)]. For data with two independent variables, we used two-way ANOVA plus Tukey's multiple comparisons test (Fig. 1A, C, H; Fig. 2C). Outliers were assessed by the ROUT test (Q=1%) and excluded for analysis. For simplicity, in Fig. 1A only statistically-significant between-genotype differences within each zone are shown.

Data availability
All data supporting the findings of this study are available within the article and its supplemental information files.

SI References

1. A. Sanchez-Lopez, *et al.*, Cardiovascular Progerin Suppression and Lamin A Restoration Rescue Hutchinson-Gilford Progeria Syndrome. *Circulation* **144**, 1777–1794 (2021).
2. M. Eriksson, *et al.*, Recurrent de novo point mutations in lamin A cause Hutchinson-Gilford progeria syndrome. *Nature* **423**, 293–298 (2003).
3. A. De Sandre-Giovannoli, *et al.*, Lamin a truncation in Hutchinson-Gilford progeria. *Science (1979)* **300**, 2055 (2003).
4. F. G. Osorio, *et al.*, Splicing-directed therapy in a new mouse model of human accelerated aging. *Sci Transl Med* **3**, 106ra107 (2011).
5. L. G. Fong, *et al.*, Prelamin A and lamin A appear to be dispensable in the nuclear lamina. *J Clin Invest* **116**, 743–752 (2006).
6. I. C. Lopez-Mejia, *et al.*, Antagonistic functions of LMNA isoforms in energy expenditure and lifespan. *EMBO Rep* **15**, 529–539 (2014).
7. L. W. Koblan, *et al.*, In vivo base editing rescues Hutchinson-Gilford progeria syndrome in mice. *Nature* **589**, 608–614 (2021).
8. M. B. Cubria, *et al.*, Evaluation of musculoskeletal phenotype of the G608G progeria mouse model with lonafarnib, pravastatin, and zoledronic acid as treatment groups. *Proc Natl Acad Sci U S A* **117**, 12029–12040 (2020).

9. I. Sörensen, R. H. Adams, A. Gossler, DLL1-mediated Notch activation regulates endothelial identity in mouse fetal arteries. *Blood* **113**, 5680–8 (2009).
10. A. Barettino, I. Benedicto, V. Andres, Whole Mount Preparation of Mouse Aorta for Confocal Microscopy Studies of the Intima. *Methods Mol Biol* **2419**, 597–610 (2022).
11. J. Schindelin, *et al.*, Fiji: an open-source platform for biological-image analysis. *Nat Methods* **9**, 676–82 (2012).
12. A. Daugherty, *et al.*, Recommendation on Design, Execution, and Reporting of Animal Atherosclerosis Studies: A Scientific Statement From the American Heart Association. *Arterioscler Thromb Vasc Biol* **37**, e131–e157 (2017).
13. M. Denis, *et al.*, Gene inactivation of proprotein convertase subtilisin/kexin type 9 reduces atherosclerosis in mice. *Circulation* **125**, 894–901 (2012).
14. M. M. Bjørklund, *et al.*, Induction of atherosclerosis in mice and hamsters without germline genetic engineering. *Circ Res* **114**, 1684–9 (2014).
15. M. R. Hamczyk, *et al.*, Vascular Smooth Muscle-Specific Progerin Expression Accelerates Atherosclerosis and Death in a Mouse Model of Hutchinson-Gilford Progeria Syndrome. *Circulation* **138**, 266–282 (2018).
16. R. M. Nevado, M. R. Hamczyk, P. Gonzalo, M. J. Andres-Manzano, V. Andres, Premature Vascular Aging with Features of Plaque Vulnerability in an Atheroprone Mouse Model of Hutchinson-Gilford Progeria Syndrome with Ldlr Deficiency. *Cells* **9** (2020).